

# Unrolling worms: Genome Editing to Rewrite Roller Phenotypes in *C. elegans*

Sohitri Mukherjee<sup>1</sup>, Andrea KH Stavoe<sup>1§</sup>

<sup>1</sup>Neurobiology and Anatomy, The University of Texas Health Science Center at Houston, Houston, TX, US

<sup>§</sup>To whom correspondence should be addressed: [andrea.k.stavoe@uth.tmc.edu](mailto:andrea.k.stavoe@uth.tmc.edu)

## Abstract

The gain-of-function allele [rol-6\(su1006\)](#) has been used as a co-injection marker to visually identify transgenic progeny following microinjection in [Caenorhabditis elegans](#). The [rol-6\(gf\)](#) allele yields a clear, visual roller phenotype; however, affected worms are twisted along the anterior-posterior axis, obscuring tissues and complicating visual analyses. We deployed CRISPR/Cas9 to “unroll” transgenic worm strains harboring [rol-6\(gf\)](#). We discovered that our successfully unrolled strains introduced additional nucleotides into the [rol-6\(gf\)](#) loci, rendering the [rol-6\(gf\)](#) copies inactive. Our results indicate that genome engineering can be easily deployed to modify existing transgenic worm strains and could be applied to other gain-of-function co-injection markers.

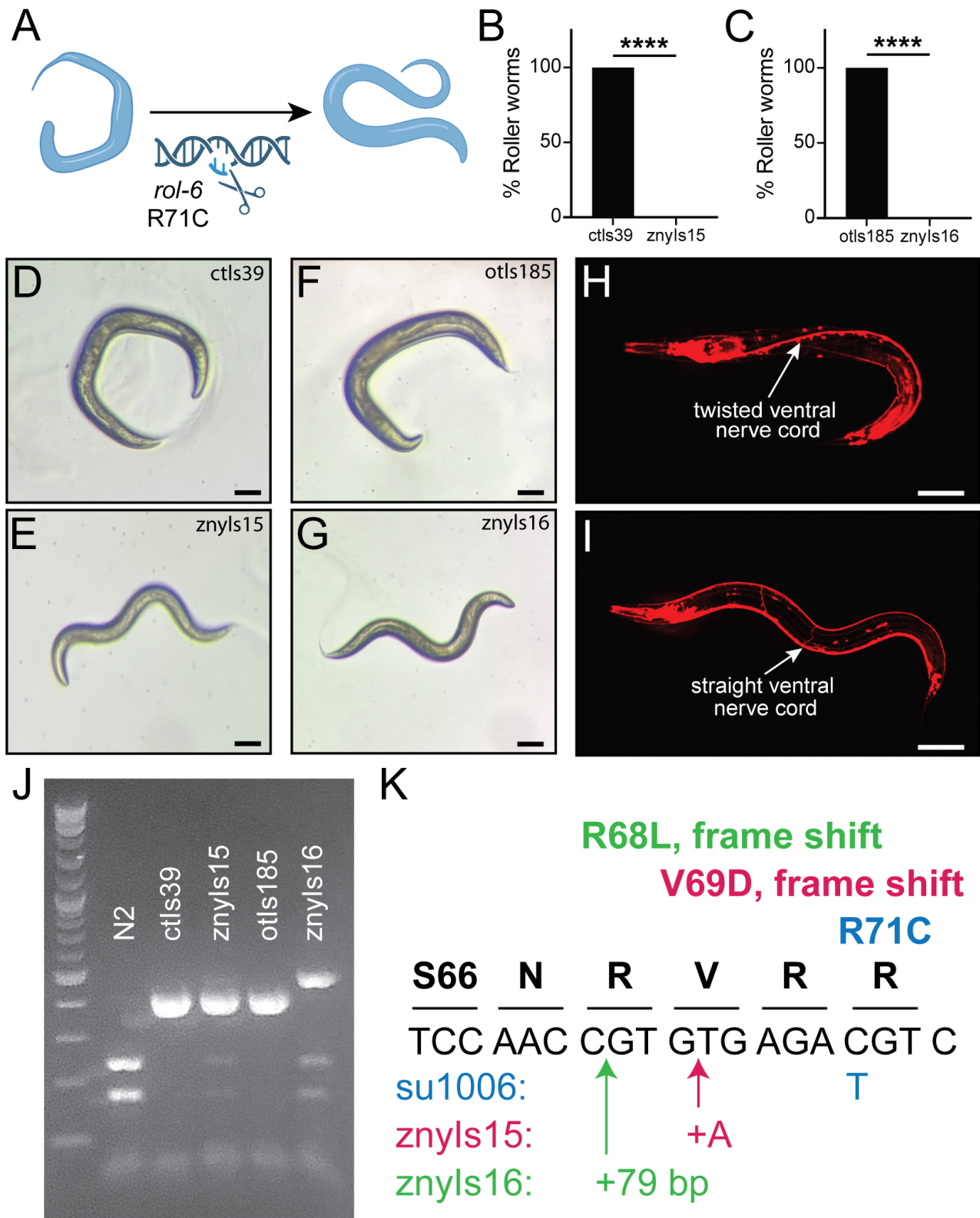


**Figure 1. Unrolling worms:**

(A) Schematic of unrolling technique. (B-C) Quantification of roller phenotype in original and unrolled strains.  $N \geq 287$  worms across three separate days of quantification for each strain. \*\*\*\*  $p < 0.0001$  by two-tailed Fisher's exact test. (D-G) Representative images of original (D, F) and unrolled worms (E, G). Scale bars, 100  $\mu$ m. (H-I) Representative micrographs of the nervous system in original (H) and unrolled worms (I). Scale bars, 50  $\mu$ m. (J) Genotyping gel for *rol-6*(*su1006*). Lane 1 is 1kb plus DNA ladder from NEB. (K) Schematic of *rol-6* sequence in front of R71. Wild type *rol-6* nucleotide sequence in black font; corresponding *ROL-6* amino acids in bold above codons. Nucleotide changes below wild type *rol-6* sequence: for *su1006* in blue, for *znyls15* in magenta, and for *znyls16* in green (79 bp inserted sequence):

tgacacctccatgtctcacagaacaccagtgacctggacacctcacaccggatggatcgtaaccggatgga). Location of nucleotide insertions are depicted by arrows. Associated amino acid changes are depicted above wild type amino acid sequence in corresponding colors.

## Description

The ease of generating transgenic worms has been an important advantage in *C. elegans* for decades. Prior to the use of fluorophores as co-injection markers, two popular co-injection strategies took advantage of whole-body phenotypes induced by single point mutations. One strategy used wild-type genes to rescue visible loss-of-function phenotypes. Two examples of this rescuing strategy include *pha-1(wt)* rescue of *pha-1(e2123ts)* (Granato et al., 1994) and *unc-119(wt)* rescue of *unc-119(ed3)* (Maduro and Pilgrim, 1995; Praitis et al., 2001). A second strategy used gain-of-function alleles that induced visible phenotypes injected into wild-type animals. One example of this second strategy is *rol-6(su1006)* to induce a roller phenotype (Kramer et al., 1990; Mello et al., 1991). These strategies either require injecting into mutant animals, which can be challenging, or generating mutant animals, which can affect worm health or the ability to visualize specific phenotypes. Many of these transgenic lines were converted into integrated strains that remain useful today, particularly if the co-injection, whole-animal phenotypes could be removed.

The *rol-6(su1006)* gain-of-function allele, as its name suggests, induces worms to roll (Cox et al., 1980; Park and Horvitz, 1986; Chen et al., 2003; Thein et al., 2003). The *rol-6(su1006)* mutation also induces a developmental delay (Sparling et al., 2023) and lower mating efficiency in males (Evans, 2006). Larval lineage tracing is more difficult in *rol-6(su1006)* larva due to their twisted cuticle (Evans, 2006). In addition, for experiments that involve visualizing the worm nervous system, the ventral nerve cord becomes more difficult to visualize in *rol* worms than in wild-type animals.

The advent of CRISPR-Cas9 gene editing now makes it possible to engineer single point mutations with surgical precision. CRISPR-Cas9 gene editing has been extensively used in *C. elegans* to edit single loci in animals, with a guide RNA targeting a single locus in the worm genome (Cho et al., 2013; Arribere et al., 2014; Zhao et al., 2014; Paix et al., 2015; Prior et al., 2017; Dokshin et al., 2018). In addition, the SKI LODGE system developed by the Mair lab uses the popular *dpy-10(cn64)* guide RNA to target the endogenous copy of *dpy-10* as the co-injection marker and an inserted copy of the *dpy-10* guide sequence to edit the SKI LODGE cassette inserted at a safe harbor locus (Silva-García et al., 2019). Thus, efficient guide RNAs can simultaneously target more than one locus in a genome.

We asked whether we could use CRISPR-Cas9 to “un-roll” roller worms made with traditional microinjection techniques. Traditional microinjection techniques generate extrachromosomal arrays that contain many copies of both the experimental plasmid and the co-injection plasmid. Thus, worms with integrated *rol-6(gf)* arrays contain an unknown, but likely high, number of *rol-6(gf)* copies that would need to be reverted to wild-type during “un-rolling.” CRISPR/Cas9 broadly involves two steps: a guide RNA targets the Cas9 enzyme to a specific location to induce a double-strand DNA break and an exogenous repair template provides the sequence to the endogenous repair machinery to generate the desired edit via homologous recombination (Arribere et al., 2014; Zhao et al., 2014; Paix et al., 2015; Prior et al., 2017; Dokshin et al., 2018). We designed a guide RNA targeted to the *rol-6(su1006)* allele and a repair template to replace *rol-6(gf)* with wild-type *rol-6*. Importantly, in the unlikely event that the endogenous *rol-6* locus were targeted, the repair template should have replaced that edit with wild-type *rol-6* (Figure 1A).

We used ribonucleoprotein-complex CRISPR-Cas9 following established methods to introduce the RNA and Cas9 protein via microinjection into adult roller *BW1932* (genotype *ctIs39*) worms (Fay et al., 1999). We chose the healthiest line of normally-moving worms and assigned this gene-edited strain a new genotype: *znyIs15 (\*ctIs39)*. We quantified the number of worms that displayed wild-type versus roller phenotypes in both the *ctIs39* and *znyIs15* worms. We found that while 100% of *ctIs39* worms exhibited roller movement, the unrolled *znyIs15* worms all displayed wild-type, sinusoidal movement (Figure 1B, 1D-E). Finally, we genotyped *znyIs15* worms for *rol-6(su1006)* to determine if all *rol-6* array copies were reverted to wild-type. We were surprised to find that our unrolled *znyIs15* DNA only displayed a faint WT band (Figure 1J). Perplexed, we then sequenced the *znyIs15 rol-6* genotyping PCR product. We discovered that *znyIs15* worms harbored a single-nucleotide insertion near the target edit site, inducing V69D and a frame shift, resulting in an early stop codon (Figure 1K). The sequencing results suggest that for successfully unrolled worms, the repair machinery ignored the repair template and instead randomly inserted a nucleotide during repair of the majority of array copies of *rol-6*. Further, it appears that this insertion occurred in multiple copies of *rol-6(gf)* within the array and likely inactivates most of the array copies of *rol-6*. These inactivated copies *rol-6*, combined with a few reverted WT *rol-6* edits, resulted in unrolled worms.

To ensure that this strategy is possible across roller strains developed by different labs, we next unrolled an independent roller strain (*OH6020*; genotype *otIs185*) (Sarin et al., 2007). Following the same protocol, we were again able to isolate unrolled worms after CRISPR-Cas9 gene editing, assigning this gene-edited strain the genotype *znyIs16 (\*otIs185)*. Similar to our previous quantifications, we found that the unrolled *znyIs16* worms completely lost the roller phenotype of *otIs185* worms (Figure 1C, 1F-G). We also genotyped *znyIs16* animals for *rol-6(su1006)*, again finding that unrolled *znyIs16* DNA only displayed a faint WT band and a larger-than-expected PCR product (Figure 1J). Similar to our *znyIs15*

sequencing results, we identified a 79-base pair insertion near the edit site in znyIs16 worms. This insertion induced R68L and a frame shift (Figure 1K), again generating an early stop codon and likely inactivating most of the array copies of [rol-6](#). As with znyIs15, a small fraction of array copies of [rol-6](#) in znyIs16 do appear to have been reverted to WT. Together, our data indicate that the guide RNA successfully targeted Cas9 to [rol-6\(gf\)](#) loci, but that we chose a suboptimal repair strategy. These results indicate that we can use CRISPR-Cas9 to unroll worms with roller phenotypes induced by the [rol-6\(su1006\)](#) gain-of-function allele, but that unrolling worms appears to be more successful by inactivating the array copies of [rol-6\(gf\)](#) than by reverting them to wild type [rol-6](#).

We next validated the utility of unrolling worms by visualizing the ventral nerve cord in unrolled worms by generating transgenic lines labeling the nervous system with [prab-3::mCherry](#). Indeed, unrolled worms displayed the typical, wild type untwisted ventral nerve cords that were easier to visualize with confocal microscopy than their roller counterparts (Figure 1H-I). These data indicate that we can unroll worm strains initially generated with roller co-injection markers instead of laboriously remaking integrated strains with different co-injection markers.

Our data show that CRISPR-Cas9 can be successfully used to edit multiple copies of [rol-6\(su1006\)](#) in *C. elegans*, including many copies of [rol-6\(gf\)](#) in multicopy arrays following microinjection and integration. Co-injection markers serve an important purpose in many transgenic strains: they identify the desired transgenic array during crossing and maintenance. Some transgenic arrays are only identifiable via their co-injection markers with a conventional, dissection microscope. Thus, some strains harboring [rol-6\(gf\)](#) co-injection markers may not be easy to work with once unrolled. This is strain-dependent, as we found that we can visualize the GFP signal of [ctIs39/znyIs15](#) with a fluorescent dissection microscope. One way to address this limitation would be to intentionally insert a cassette into the repair template that could be identified by PCR-based genotyping, similar to the cassette we unintentionally inserted to yield znyIs16. Together, our results identify a new CRISPR-based method to easily revert phenotype-causing [rol-6\(gf\)](#) point mutations from existing transgenic worm strains. This theory may also be applied to other gain-of-function co-injection markers.

## Methods

### Genome editing

The [rol-6\(su1006\)](#) guide RNA (crRNA) and repair template (HDR, ssODN) were designed using Integrated DNA Technologies (IDT) Alt-R™ HDR Design Tool (<https://www.idtdna.com/site/order/designtool/index/HDRDESIGN>).

znyIs15 and znyIs16 were generated using an adapted CRISPR protocol (Ghanta and Mello, 2020). Briefly, the [rol-6\(su1006\)](#) crRNA, tracrRNA, and Cas9 protein were mixed and injected into [BW1932](#) and [OH6020](#) adult worms. All CRISPR reagents were obtained from IDT.

Injected worms were singled onto plates and allowed to recover and lay eggs for three days. Then, plates were examined for normal-moving progeny. All normal-moving progeny were singled onto new plates. After another three days, plates were examined for F2 progeny that exhibited normal sinusoidal movement. The healthiest line for each “un-rolling” was selected for subsequent experiments.

### Quantifying rol phenotype

We counted L4-adult worms freely moving on plates with [OP50](#) lawns, assaying worms for the roller phenotype versus sinusoidal movement. Approximately 100 worms were quantified per genotype per session. Worms were quantified on three separate sessions on different days.

### Transgenesis

Transgenic worms were generated following established techniques. pwAS70 [[rab-3p::mCh](#)] and pwAS1 [[unc-122p::gfp](#)] were co-injected at 5ng/uL and 30 ng/uL, respectively, into [N2](#) or [VOE643](#) worms to generate znyEx214 and znyEx220, respectively. znyEx214 was crossed to [otIs185](#) to generate [VOE689](#).

### Microscopy

For white-light images, worms were left on agar with [OP50](#). Worms were imaged on a dissection microscope at 25x magnification. Images were captured with an iPhone. Images were cropped and rotated in FIJI.

For fluorescent images, worms were mounted on 2% agarose pads and immobilized in 10 mM levamisole (Sigma 31742-250MG). Worms were imaged on a spinning disk confocal microscope (Nikon Ti2 Inverted Confocal with Yokogawa W1 Spinning Disk Package, Nikon Instruments) with a CFI super fluor 40x, 1.3 NA oil immersion objective (Nikon Instruments). Z-stack digital micrographs (step size: 0.5 microns) were acquired with a back-illuminated cCMOS camera (Teledyne Photometrics) using Nikon Elements software (Nikon Instruments).

### Statistics

We performed two-tailed Fisher's exact tests with Prism 10 (GraphPad).

## Reagents

### Strain table

Strain	Genotype	Available From
<a href="#">N2</a>	Wild type	CGC
<a href="#">BW1932</a>	<a href="#">ctIs39</a>	CGC
<a href="#">OH6020</a>	<a href="#">otIs185</a>	CGC
<a href="#">VOE641</a>	znyIs15 (* <a href="#">ctIs39</a> )	Stavoe lab
<a href="#">VOE643</a>	znyIs16 (* <a href="#">otIs185</a> )	Stavoe lab
<a href="#">VOE671</a>	znyEx214 [ <a href="#">rab-3p</a> ::mCh (5 ng/uL), <a href="#">unc-122p</a> ::gfp (30 ng/uL)]	Stavoe lab
<a href="#">VOE689</a>	znyEx214; <a href="#">otIs185</a>	Stavoe lab
<a href="#">VOE690</a>	znyEx220 [ <a href="#">rab-3p</a> ::mCh (5 ng/uL), <a href="#">unc-122p</a> ::gfp (30 ng/uL)]; znyIs16	Stavoe lab

### Plasmids

Plasmid	Genotype	Description
pwAS1	<a href="#">unc-122p</a> ::gfp:: <a href="#">unc-54</a> 3' UTR	4kb <a href="#">unc-122</a> promoter driving codon-optimized gfp, including Ce introns. Available from Addgene.
pwAS70	<a href="#">rab-3p</a> ::mCh:: <a href="#">unc-10</a> 3' UTR	4.4kb <a href="#">rab-3</a> promoter driving codon-optimized mCherry, including Ce introns. Available from Stavoe lab.

### Genotyping [rol-6](#)

[rol-6\(su1006\)](#) Fwd: CTG AAA ATT TCC AGA TGA CCC TAA CTA CGG

[rol-6\(su1006\)](#) Rev: GAA TGG ACC ATC TGG GAA TCC ACC

AatII (New England Biolabs # R3162S) cuts [N2](#) (421 and 31 bp) and [rol-6\(su1006\)](#) (242, 179 and 31 bp).

1kb plus DNA ladder (New England Biolabs).

Undigested PCR product was sent for Sanger sequencing with Quintara Biosciences.

### CRISPR-Cas9 reagents

Reagent	Available From	Catalog number
Alt-R S.p. Cas9 Nuclease V3, 100ug (Cas9 protein)	IDT	1081058
Alt-R CRISPR-Cas9 tracrRNA, 20 nmol	IDT	203459079
<a href="#">rol-6(su1006)</a> crRNA	IDT	Sequence: /A1TR1/rUrUrGrUrUrGrArCrArUrCrUrCrArCrArCrGrGrUrGrUrUrUrArGrArGrCrUrArUrGrCrU/A1TR2/

<a href="#">rol-6</a> (wt) HDR (ssODN) (plus strand)	IDT	Sequence: /AIT-R-HDR1/G*T*TGATATGGTTAACTTGGAG CAGGAACCGCTTCCAACCGTGTGAGACGTCAACAATATGG AGGATATGGAGCCACTGGTGTTCAG*C*C/AIT-R-HDR2/
---	-----	--

### Software

ImageJ (NIH) (Schindelin et al., 2012); Prism 10 (Graphpad). Figure was assembled using Adobe Illustrator.

**Acknowledgements:** We thank members of the Arey, Stavoe, and Waxham labs for their thoughtful comments.

Some strains were provided by the CGC, which is funded by NIH Office of Research Infrastructure Programs (P40 OD010440).

### **References**

- Arribere JA, Bell RT, Fu BX, Artiles KL, Hartman PS, Fire AZ. 2014. Efficient marker-free recovery of custom genetic modifications with CRISPR/Cas9 in *Caenorhabditis elegans*. *Genetics* 198(3): 837-46. PubMed ID: [25161212](#)
- Chen S, Spence AM, Schachter H. 2003. Isolation of null alleles of the *Caenorhabditis elegans* gly-12, gly-13 and gly-14 genes, all of which encode UDP-GlcNAc: alpha-3-D-mannoside beta1,2-N-acetylglucosaminyltransferase I activity. *Biochimie* 85(3-4): 391-401. PubMed ID: [12770777](#)
- Cho SW, Lee J, Carroll D, Kim JS, Lee J. 2013. Heritable gene knockout in *Caenorhabditis elegans* by direct injection of Cas9-sgRNA ribonucleoproteins. *Genetics* 195(3): 1177-80. PubMed ID: [23979576](#)
- Cox GN, Laufer JS, Kusch M, Edgar RS. 1980. Genetic and Phenotypic Characterization of Roller Mutants of *CAENORHABDITIS ELEGANS*. *Genetics* 95(2): 317-39. PubMed ID: [17249038](#)
- Dokshin GA, Ghanta KS, Piscopo KM, Mello CC. 2018. Robust Genome Editing with Short Single-Stranded and Long, Partially Single-Stranded DNA Donors in *Caenorhabditis elegans*. *Genetics* 210(3): 781-787. PubMed ID: [30213854](#)
- Evans T. 2006. Transformation and microinjection. *WormBook* : 10.1895/wormbook.1.108.1. DOI: [doi/10.1895/wormbook.1.108.1](#)
- Fay DS, Stanley HM, Han M, Wood WB. 1999. A *Caenorhabditis elegans* homologue of hunchback is required for late stages of development but not early embryonic patterning. *Dev Biol* 205(2): 240-53. PubMed ID: [9917360](#)
- Ghanta KS, Mello CC. 2020. Melting dsDNA Donor Molecules Greatly Improves Precision Genome Editing in *Caenorhabditis elegans*. *Genetics* 216(3): 643-650. PubMed ID: [32963112](#)
- Granato M, Schnabel H, Schnabel R. 1994. pha-1, a selectable marker for gene transfer in *C. elegans*. *Nucleic Acids Res* 22(9): 1762-3. PubMed ID: [8202383](#)
- Kramer JM, French RP, Park EC, Johnson JJ. 1990. The *Caenorhabditis elegans* rol-6 gene, which interacts with the sqt-1 collagen gene to determine organismal morphology, encodes a collagen. *Mol Cell Biol* 10(5): 2081-9. PubMed ID: [1970117](#)
- Maduro M, Pilgrim D. 1995. Identification and cloning of unc-119, a gene expressed in the *Caenorhabditis elegans* nervous system. *Genetics* 141(3): 977-88. PubMed ID: [8582641](#)
- Mello CC, Kramer JM, Stinchcomb D, Ambros V. 1991. Efficient gene transfer in *C.elegans*: extrachromosomal maintenance and integration of transforming sequences. *EMBO J* 10(12): 3959-70. PubMed ID: [1935914](#)
- Paix A, Folkmann A, Rasoloson D, Seydoux G. 2015. High Efficiency, Homology-Directed Genome Editing in *Caenorhabditis elegans* Using CRISPR-Cas9 Ribonucleoprotein Complexes. *Genetics* 201(1): 47-54. PubMed ID: [26187122](#)
- Park EC, Horvitz HR. 1986. Mutations with dominant effects on the behavior and morphology of the nematode *Caenorhabditis elegans*. *Genetics* 113(4): 821-52. PubMed ID: [3744028](#)
- Praitis V, Casey E, Collar D, Austin J. 2001. Creation of low-copy integrated transgenic lines in *Caenorhabditis elegans*. *Genetics* 157(3): 1217-26. PubMed ID: [11238406](#)
- Prior H, Jawad AK, MacConnachie L, Beg AA. 2017. Highly Efficient, Rapid and Co-CRISPR-Independent Genome Editing in *Caenorhabditis elegans*. *G3 (Bethesda)* 7(11): 3693-3698. PubMed ID: [28893845](#)
- Sarin S, O'Meara MM, Flowers EB, Antonio C, Poole RJ, Didiano D, et al., Hobert O. 2007. Genetic screens for *Caenorhabditis elegans* mutants defective in left/right asymmetric neuronal fate specification. *Genetics* 176(4): 2109-30. PubMed ID: [17717195](#)

Schindelin J, Arganda-Carreras I, Frise E, Kaynig V, Longair M, Pietzsch T, et al., Cardona A. 2012. Fiji: an open-source platform for biological-image analysis. *Nat Methods* 9(7): 676-82. PubMed ID: [22743772](#)

Silva-García CG, Lanjuin A, Heintz C, Dutta S, Clark NM, Mair WB. 2019. Single-Copy Knock-In Loci for Defined Gene Expression in *Caenorhabditis elegans*. *G3 (Bethesda)* 9(7): 2195-2198. PubMed ID: [31064766](#)

Sparling AC, King DE, Meyer JN. 2023. *rol-6* and *dpy-10* *C. elegans* mutants have normal mitochondrial function after normalizing to delayed development. *MicroPubl Biol* 2023: 10.17912/micropub.biology.000798. PubMed ID: [37215639](#)

Thein MC, McCormack G, Winter AD, Johnstone IL, Shoemaker CB, Page AP. 2003. *Caenorhabditis elegans* exoskeleton collagen COL-19: an adult-specific marker for collagen modification and assembly, and the analysis of organismal morphology. *Dev Dyn* 226(3): 523-39. PubMed ID: [12619137](#)

Zhao P, Zhang Z, Ke H, Yue Y, Xue D. 2014. Oligonucleotide-based targeted gene editing in *C. elegans* via the CRISPR/Cas9 system. *Cell Res* 24(2): 247-50. PubMed ID: [24418757](#)

**Funding:** This work was supported by R35-GM159826 to AKHS.

Supported by National Institute of General Medical Sciences (United States) R35-GM159826 to Andrea KH Stavoe.

**Conflicts of Interest:** The authors declare that there are no conflicts of interest present.

**Author Contributions:** Sohriti Mukherjee: investigation, formal analysis, writing - review editing. Andrea KH Stavoe: conceptualization, funding acquisition, methodology, investigation, writing - original draft, writing - review editing.

**Reviewed By:** Anonymous

**Nomenclature Validated By:** Anonymous

**WormBase Paper ID:** WBPaper00069895

**History:** Received May 5, 2026 **Revision Received** June 6, 2026 **Accepted** June 29, 2026 **Published Online** June 30, 2026 **Indexed** July 14, 2026

**Copyright:** © 2026 by the authors. This is an open-access article distributed under the terms of the Creative Commons Attribution 4.0 International (CC BY 4.0) License, which permits unrestricted use, distribution, and reproduction in any medium, provided the original author and source are credited.

**Citation:** Mukherjee S, Stavoe AK. 2026. Unrolling worms: Genome Editing to Rewrite Roller Phenotypes in *C. elegans*. *microPublication Biology*. [10.17912/micropub.biology.002185](#)